Elastic Wave Field Neural Networks for Structural Health Monitoring: An Analytical and Numerical Study of Multiple Neurons

Arata Masuda[1], and Konosuke Takashima[2]

[1] *Faculty of Mechanical Engineering, Kyoto Institute of Technology, Matsugasaki, Sakyo-ku, Kyoto, 606-8585, Japan*
masuda@kit.ac.jp

[2] *Division of Mechanophysics, Kyoto Institute of Technology*
m3623016@edu.kit.ac.jp

ABSTRACT

The purpose of this study is to develop a novel concept of smart structural systems recognizing their own structural integrity by an embodied high density sensor network. In our concept, a number of sensor nodes are embedded in the host structure, each of which reacts pointwise to the structural vibration with a simple rule. This allows the whole nodes to be mutually coupled through the elastic field, forming a neural network that incorporates the dynamic characteristics of the host structure as the coupling weights. In the previous study, we presented that a single-neuron network as its minimum configuration can exhibit a bifurcation of its dynamics behavior, which can be used to detect the change of the network due to damages. In this study, the formulation of networks with multiple neurons deployed in a structure with single-mode approximation is presented particularly focusing on the bifurcation analysis to reveal how the behavior of the network is drastically altered depending of the network and structural parameters. Numerical analysis is conducted to examine the validity of the bifurcation analysis.

1. INTRODUCTION

Structural health monitoring (SHM) technology, which aims to continuously, automatically, and remotely monitor the healthiness of structures, was proposed in the 1990s to reduce structural maintenance costs. It has become more and more realistic since the 2000s, when rapid advances in wireless sensor network technology made it possible to acquire large amounts of data using sensors densely embedded in structures. In fact, it has now become reasonable to deploy 1000 sensor nodes in a single structural system.

Typical sensor networks have a star or tree topology. Data are collected at every sensor node and aggregated via these communication links in one place to perform signal processing and diagnostic algorithms. This is a centralized approach, in which the communication and computational costs associated with the concentration of data can be problematic as the increase of the sensor nodes and more use of higher frequency dynamical data (vibrations and waves) to perform early detection of structural damage. Therefore, it is obvious that further increase of sensor density will saturate the network bandwidth and capacity of centralized computational resources (Abdulkarem, Samsudin, Rokhani, & A Rasid, 2019).

One promising solution, as the second approach, to reduce the burden on the wireless communication channel and computational resources due to data concentration would be edge computing. In this approach, the network is hierarchized, and computational resources are allocated to intermediate nodes close to the structure. This allows primary processing of data to be performed locally, to transmit features, the higher-order information extracted from the data, to higher-level nodes instead of sending the raw data though the communication channel. However, this approach does not change the fact that data is still collected at the local node, and having some rich computational resources locally may increase the cost of power supply and maintenance, which prevents this approach from being truly scalable.

As the third approach, the authors proposed to use the structure itself as a computational resource to realize a truly scalable sensor network (Masuda, Sakai, & Takashima, 2023; Masuda, Takashima, & Sakai, 2023). This is done by building a kind of neural network on the structure, hereafter referred to as elastic wave field neural network (EWFNN), using the elastic wave field as a medium, so that the structure itself acquires an intelligent function to recognize its own healthiness (Masuda, Sakai, & Takashima, 2023). Analogically speaking, this is like building a “brain” function parasitically on the structure, whereas the conventional SHM sensor network is like placing it outside the structure (Fig. 1).

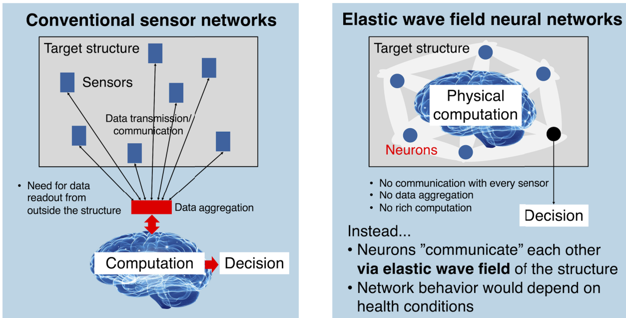

Figure 1. Concept of EWFNN-based SHM.

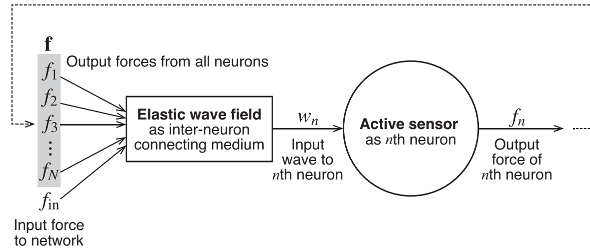

Figure 2. Structure of EWFNN.

Specifically, we consider a large number of active sensor nodes deployed on the structure as neurons. One node performs as both a sensor and an actuator, and reads the elastic wave propagating through the structure as an input and outputs it as an excitation force to the structure after performing a nonlinear activation function (Fig. 2). This means that these neurons form a Hopfield-type fully-connected neural network coupled via the elastic wave field of the host structure. In the previous paper (Masuda, Sakai, & Takashima, 2023), we designed a EWFNN operating in a single frequency, in which all neurons operate in the same frequency with slowly varying amplitude and phase. The operation of the neuron is then regarded as a nonlinear dynamical system of the complex amplitude, and the connection between arbitrary two neurons is represented by a complex weight, i.e., the value of the frequency response function (FRF) between them at the operating frequency.

Since the FRF between neurons act as the connection weights in this network, the behavior of the network essentially reflects the dynamic characteristics of the structure. Therefore, the entire network can function as a damage detector only relying on simple and independent calculation, not referring to the internal states of other neurons if the network behavior drastically change with the presence of the damage. In the previous paper (Masuda, Sakai, & Takashima, 2023), it was presented that the network can be designed so that it yields a bifurcation caused by the damage. This can be a major advantage over the conventional sensor network-based SHM approaches because it does not require inter-neuron data transmission or data aggregation to perform damage detection algorithms.

The previous study presented the formulation of EWFNN driven by a single-frequency excitation, particularly focusing on a single-neuron network as the smallest configuration (Masuda, Sakai, & Takashima, 2023). In this study, the formulation and analysis are extended to multiple-neuron configuration, assuming single-mode operation. Equilibrium analysis is performed to derive a simple criterion of Hopf bifurcation of the complex amplitude due to damage, which corresponds to the change from modulated response to steady-state, and to discuss how the existence of multiple neurons can contribute to the detection of local damage. Numerical experiments are presented to validate the analytical findings using a single-mode model of a thin plate structure.

2. FORMULATION

2.1. Modeling of neurons operating in single frequency

The basic formulation of EWFNNs presented in the previous study (Masuda, Sakai, & Takashima, 2023) is briefly summarized in this section. The EWFNN operating under a single sinusoidal excitation with an operating frequency of ω_o can be treated as a continuous-time dynamical system of slowly varying complex amplitudes of the input and output of neurons, of which absolute value and argument represent slowly varying real amplitude and phase, respectively. Let w_n, f_n, and f_in be the input and output of nth neuron, and the input force exciting the network, respectively. Then, the slow dynamics assumption allows us to represent them as

$$w_n(t) = \hat{w}_n(t)e^{i\omega_\text{o}t},\ f_n(t) = \hat{f}_n(t)e^{i\omega_\text{o}t},\ f_\text{in}(t) = \hat{f}_\text{in}e^{i\omega_\text{o}t} \tag{1}$$

where variables with hat denote slowly varying complex amplitudes. The input-output dynamics of the nth neuron is then given by

$$\tau_n \frac{\mathrm{d}\hat{u}_n(t)}{\mathrm{d}t} + \hat{u}_n(t) = \hat{w}_n(t) + \beta_n \tag{2}$$

$$\hat{f}_n(t) = \gamma_n \tanh(\alpha_n|\hat{u}_n(t)|)\hat{u}_n(t)/|\hat{u}_n(t)| \tag{3}$$

where $\hat{u}_n$ is a complex-valued state variable, and τ_n is a time constant set much larger than $2\pi/\omega_\text{o}$ to ensure the slow dynamics of the network. Equation (3) states that the output is calculated by performing a complex split activation function classified as type B by Bassey et al. (Bassey, Qian, & Li, 2021) on the state variable, where α_n and γ_n are input and output gains, respectively. This formulation is similar to that used in the formulation of continuous-time Hopfield networks (Hopfield, 1984; Chen, Zhang, & Wang, 2004).

The dynamics of the host structure is described using the

FRFs at the operating frequency:

$$\hat{w}_n(t) = \sum_{m=1}^{N} G_{nm}(\omega_\mathrm{o})\hat{f}_m(t) + G_n^{\mathrm{in}}(\omega_\mathrm{o})\hat{f}_{in} \tag{4}$$

where $G_{nm}(\omega)$ is the FRF from the mth neuron to nth neuron, and $G_n^{\mathrm{in}}(\omega)$ is the FRF from the input force to nth neuron. From Eqs. (2), (3), and (4), one can obtain the state equations, i.e., differential equations of neuron dynamics, as

$$\begin{aligned}\tau_n \frac{\mathrm{d}\hat{u}_n(t)}{\mathrm{d}t} &+ \hat{u}_n(t)\\ &= \sum_{m=1}^{N} G_{nm}(\omega_\mathrm{o})\gamma_m \tanh(\alpha_m|\hat{u}_m(t)|)\frac{\hat{u}_m(t)}{|\hat{u}_m(t)|}\\ &\quad + G_n^{\mathrm{in}}(\omega_\mathrm{o})\hat{f}_{in} + \beta_n \quad (n = 1, \ldots, N)\end{aligned} \tag{5}$$

Similar to the previous study, the bias β is supposed to be trained in the training phase such that

$$\beta_n = -G_n^{\mathrm{in}}(\omega_\mathrm{o})\hat{f}_{in} \tag{6}$$

This is easily done by setting the output gain γ_n to zero, and adjusting β_n such that the state variable $\hat{u}_n$ vanishes.

2.2. Bifurcation analysis for multiple-neuron network on single-mode host structure

Let us first assume that the host structure is operated in a specific single mode, and all the neurons have the same time constant τ. Then, the state variables of all the neurons can be represented in the one-dimensional subspace that the mode shape of the target mode spans as

$$\hat{u}_n(t) = \phi_n \hat{\xi}(t) \tag{7}$$

where ϕ_n is the mode shapes of the target mode at the location of the nth neuron, and $\hat{\xi}$ is the reduced state variable in the modal coordinate. Furthermore, assuming that the neuron's input is the displacement, or its spatial derivatives, the FRF is specified in the form of

$$G_{nm} = \lambda(\omega_\mathrm{o})\phi_n\phi_m \tag{8}$$

where

$$\lambda(\omega) = \frac{\frac{1}{m_k}}{-\omega^2 + 2i\zeta_k\omega_k\omega + {\omega_k}^2} \tag{9}$$

where ω_k, ζ_k, and m_k are the natural frequency, damping ratio, and modal mass of the target mode, respectively.

Substituting Eqs. (6), (7) and (8) into Eq. (5) leads to a reduced-order state equation in the modal coordinate

$$\begin{aligned}\tau \frac{\mathrm{d}\hat{\xi}(t)}{\mathrm{d}t} &+ \hat{\xi}(t)\\ &= \lambda(\omega_\mathrm{o}) \sum_{n=1}^{N} \gamma_n|\phi_n| \tanh(\alpha_n|\phi_n||\hat{\xi}(t)|)\frac{\hat{\xi}(t)}{|\hat{\xi}(t)|}\end{aligned} \tag{10}$$

This equation gives an autonomous system that rules the behavior of all neurons in the network.

In order to understand the asymptotic behavior of this network, the autonomous system Eq. (10) is analyzed in terms of its equilibria and stability. First, the state variable $\hat{\xi}$ is represented in a polar form as

$$\hat{\xi}(t) = a(t)e^{i\theta(t)} \tag{11}$$

Substituting it into Eq. (10) followed by multiplying $e^{-i\theta(t)}$ leads to

$$\tau\left(\frac{\mathrm{d}a(t)}{\mathrm{d}t} + ia(t)\frac{\mathrm{d}\theta(t)}{\mathrm{d}t}\right) + a(t) = \lambda(\omega_\mathrm{o})\psi(a(t)) \tag{12}$$

where ψ is the amplitude activation function in the modal coordinate defined as

$$\psi(a) = \sum_{n=1}^{N} \gamma_n|\phi_n| \tanh(\alpha|\phi_n|a) \tag{13}$$

Finally, dividing above equation into real and imaginary parts gives

$$\tau\frac{\mathrm{d}a(t)}{\mathrm{d}t} + a(t) = \mathrm{Re}\left[\lambda(\omega_\mathrm{o})\right]\psi(a(t)) \tag{14}$$

$$\tau\frac{\mathrm{d}\theta(t)}{\mathrm{d}t} = \frac{1}{a(t)}\mathrm{Im}\left[\lambda(\omega_\mathrm{o})\right]\psi(a(t)) \tag{15}$$

The above system of equations is a straightforward extension of the equations for the single-neuron configuration (Masuda, Sakai, & Takashima, 2023). Similarly, Eq. (14) is a real-valued scalar homogeneous differential equation of amplitude, and Eq. (15) can be solved by substituting the solution of Eq. (14) and integrating it.

The modal activation function ψ is a wighted sum of the activation functions ($\tanh$) of all neurons, thus, it inherits the properties of $\tanh$, i.e., monotonically increasing starting from the origin, convex upward, and saturated. These properties allows the similar bifurcation analysis of Eq. (14), which concludes that the network has two operation modes with different attractors:

when $\mathrm{Re}\left[\lambda(\omega_\mathrm{o})\right]\psi'(0) > 1$,
it has a limit cycle $\hat{\xi}(t) = a_\mathrm{c}e^{i(\omega_\mathrm{c}t+\theta_0)}$ as its attractor such that

$$a_\mathrm{c} = \mathrm{Re}\left[\lambda(\omega_\mathrm{o})\right]\psi(a_\mathrm{c}) \tag{16}$$

$$\omega_\mathrm{c} = \frac{1}{\tau a_\mathrm{c}}\mathrm{Im}\left[\lambda(\omega_\mathrm{o})\right]\psi(a_\mathrm{c}) \tag{17}$$

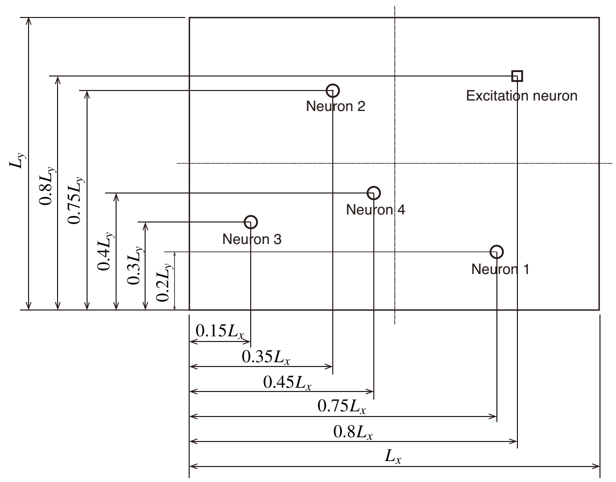

Figure 3. Top view of a rectangular plate as the target structure. All the edges are simply supported.

Table 1. Values of parameters

Description	Symbol	Value
Dimensions of plate	L_x	1.4
	L_y	1
Natural frequency of (2,2) mode	ω_k	6.04
Modal damping ratio	ζ_k	0.01
Modal mass	m_k	1
Time constant of neuron	τ	10
Input gain	α_n	2
Output gain	γ_n	1

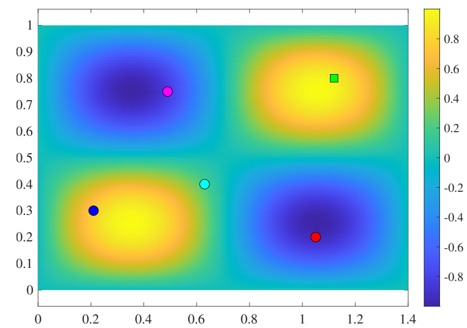

Figure 4. (2,2)-mode shape and neuron location.

thus, the response of the structure at the location of the nth neuron is derived from Eqs. (2), (6) and (7) as

$$\hat{w}(t) = (1 + i\tau\omega_c)a_c\phi_n e^{i(\omega_c t+\theta_0)} + G^{\text{in}}(\omega_o)\hat{f}_{in} \tag{18}$$

which states that the response of the structure in the time domain exhibits a modulation in amplitude and phase;

otherwise,

it has a point attractor at the origin, thus, the response of the structure at the location of the neuron is

$$\hat{w}(t) = G^{\text{in}}(\omega_o)\hat{f}_{in} \tag{19}$$

which means that the response of the structure in the time domain is steady-state, and the neuron ceases its output.

This is a Hopf bifurcation of the complex amplitude. In other words, this changes the response in the time domain from steady-state to amplitude and phase modulation. The bifurcation parameter is $\mathrm{Re}\left[\lambda(\omega_o)\right]\psi'(0)$, which is further calculated as

$$\begin{aligned}&\mathrm{Re}\left[\lambda(\omega_o)\right]\psi'(0)\\ &=\mathrm{Re}\left[\frac{\frac{1}{m_k}}{-\omega_o^2 + 2i\zeta_k\omega_k\omega_o + {\omega_k}^2}\right]\sum_{n=1}^{N}\alpha_n\gamma_n|\phi_n|^2\end{aligned} \tag{20}$$

Hence, both the global parameters (natural frequency and modal damping ratio) and local parameters (mode shapes) govern the bifurcation. This means that the local change of the mode shapes can affect the global behavior of the network.

2.3. Bifurcation-based SHM

The concept of the EWFNN-based SHM is to perform damage detection based on the behavior of the EWFNN built on the host structure. The core idea is to utilize the bifurcation between the limit cycle (modulated response) and the point attractor (steady-state response) of the network response to detect the change of the dynamics of the host structure caused by damages. The finding described above that the changes of not only the global modal parameters but also the local mode shapes can yield the global bifurcation suggests the potential benefit of the densely deployed multiple-neuron EWFNN as a damage detector. It can be more sensitive to local damages than the single-neuron network (Masuda, Sakai, & Takashima, 2023), which only has sensitivity to the global modal parameters.

3. NUMERICAL EXAMPLE

3.1. Target structure

An illustrative numerical example is presented to show the validity of the presented analysis of the bifurcation of the network behavior. A simply supported isotropic rectangular plate depicted in Fig. 3 was presumed as the target structure. Four neurons and one excitation neuron were deployed at the locations indicated in the figure. The values of the relevant parameters are listed in Table 1. Note that all the parameters are appropriately nondimensionalized.

We assumed that the dynamics of the plate is described by a single dominant mode (2,2) at the operating frequency and

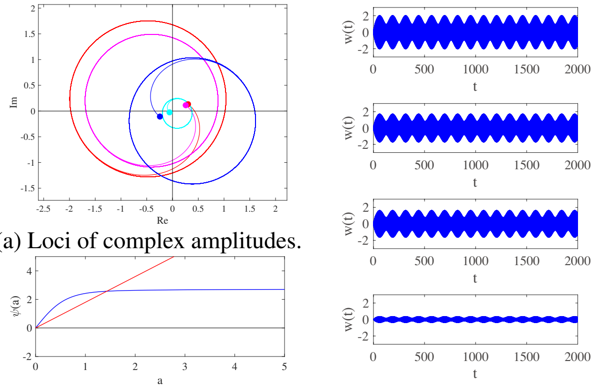

(a) Loci of complex amplitudes.

(b) Modal activation function.

(c) Temporal responses.

Figure 5. Results of numerical experiments for $\omega_{\mathbf{o}} = 0.98\omega_k$.

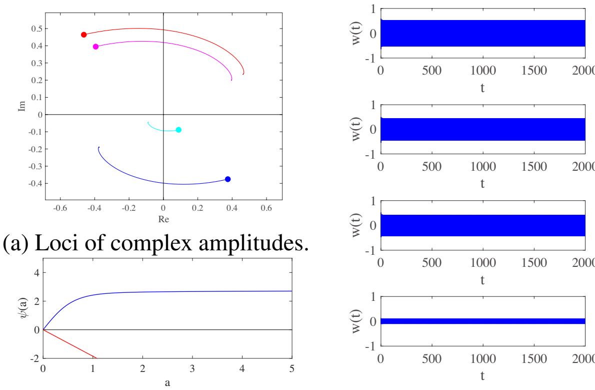

(a) Loci of complex amplitudes.

(b) Modal activation function.

(c) Temporal responses.

Figure 7. Results of numerical experiments for $\omega_{\mathbf{o}} = 1.02\omega_k$.

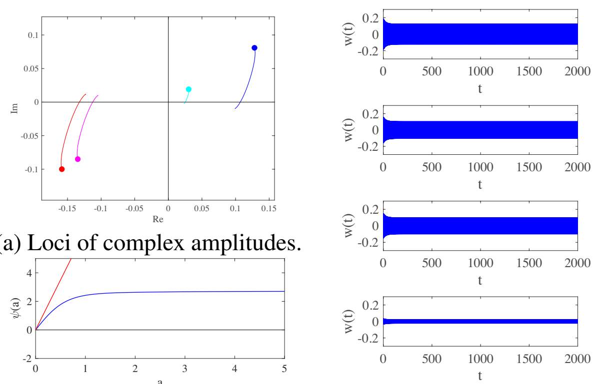

(a) Loci of complex amplitudes.

(b) Modal activation function.

(c) Temporal responses.

Figure 6. Results of numerical experiments for $\omega_{\mathbf{o}} = 0.9\omega_k$.

that the neurons measure the out-of-plane displacement of the plate as their input. The (2,2)-mode shape is shown with the location of the neurons in Fig. 4. As indicated in the figure, the neurons 1, 2, and 3 are located near the antinode of the (2,2)-mode, whereas the neuron 4 is near the nodal line.

3.2. Results

Numerical experiment was conducted for three different operating frequencies to verify the bifurcation analysis presented in the previous section. First, as the training phase, the output gain γ of the neuron was set to zero, and the bias was trained as described in Eq. (6). Then, the output gain was set to the prescribed value, and the state variables of the network were calculated by numerically integrating Eq. (5) by ode45 of MATLAB with randomly set initial values. The displacement responses at the neurons were calculated from Eq. (4).

The results are shown in Figs. 5, 6, and 7 for $\omega_{\mathrm{o}} = 0.98\omega_k$, $0.9\omega_k$, and $1.02\omega_k$. Each of figures shows (a) the loci of the complex amplitudes of the displacements at the neuron location $\hat{w}_n$, in which the colors of the lines are corresponding to the colors of the neurons depicted in Fig. 4, (b) the shape of the modal activation function $\psi(a)$ with the line of $1/\mathrm{Re}\left[\lambda(\omega_{\mathrm{o}})\right]$, and (c) the temporal responses of the displacements at the neuron locations, w_1, w_2, w_3, and w_4.

The plots clearly show that the network responses are drastically changed by the small variation of the operating frequency. The network was attracted to modulated responses, as shown in Fig. 5, because the operating frequency was set slightly below the natural frequency where the real part of the λ is greater than the threshold $1/(\psi'(0))$. In this case, the modal activation function has a stable intersection with the line of $1/\mathrm{Re}\left[\lambda(\omega_{\mathrm{o}})\right]$ at a positive value of a, which corresponds to the limit cycle amplitude a_c. In contrast, when the operating frequency moved away from the natural frequency, the network converged to a steady-state response, as shown in Figs. 6 and 7, since real part of the λ becomes smaller than the threshold $1/(\psi'(0))$. In these cases, the modal activation function has a stable intersection with the line of $1/\mathrm{Re}\left[\lambda(\omega_{\mathrm{o}})\right]$ only at the origin, which corresponds to the point attractor.

4. CONCLUSIONS

In this study, the formulation of EWFNN investigated in the previous study was extended to multiple-neuron configuration, assuming single-mode operation. The formulation of the network was presented and the equilibrium analysis was performed to derive a simple criterion of Hopf bifurcation of the complex amplitude of the state variables of the neurons due to the change of the network and structural parameters. Then, numerical analysis was conducted to examine the validity of the bifurcation analysis. The findings of the bifurcation analysis suggested the potential benefit of dense deployment of neurons in EWFNN to perform as a damage detector because the analysis concluded that the bifurcation of the network behavior can be triggered not only by the changes of global modal parameters but also by the change of local mode shapes.

Future study may include more comprehensive analysis of the sensitivity of the bifurcation to the local structural parameters and how the sensitivity can be enhanced by designing more appropriate activation function as well as the gain parameters in the neuron. Extension of the theory to multi-mode situation would be another challenge.

REFERENCES

Abdulkarem, M., Samsudin, K., Rokhani, F. Z., & A Rasid, M. F. (2019). Wireless sensor network for structural health monitoring: A contemporary review of technologies, challenges, and future direction. *Structural Health Monitoring*. doi: 10.1177/1475921719854528

Bassey, J., Qian, L., & Li, X. (2021). *A survey of complex-valued neural networks.* arXiv. doi: 10.48550/ ARXIV. 2101.12249

Chen, S., Zhang, Q., & Wang, C. (2004). Existence and stability of equilibria of the continuous-time hopfield neural network. *Journal of Computational and Applied Mathematics*, *169*(1), 117-125. doi: https://doi.org/10.1016/j.cam.2003.11.014

Hopfield, J. J. (1984). Neurons with graded response have collective computational properties like those of two-state neurons. *Proceedings of the National Academy of Sciences*, *81*(10), 3088-3092. doi: 10.1073/pnas.81.10.3088

Masuda, A., Sakai, R., & Takashima, K. (2023). Making a brain on a structure: a conceptual study of elastic wave field neural networks for structural health monitoring. In J. Yang, G. Huang, M. A. Nouh, S. Shahab, & S. Tol (Eds.), *Active and passive smart structures and integrated systems xvii* (Vol. 12483, p. 124831J). SPIE. doi: 10.1117/12.2658694

Masuda, A., Takashima, K., & Sakai, R. (2023). Physical reservoir-based structural health monitoring: a preliminary study. In J. Yang, G. Huang, M. A. Nouh, S. Shahab, & S. Tol (Eds.), *Active and passive smart structures and integrated systems xvii* (Vol. 12483, p. 1248311). SPIE. doi: 10.1117/12.2658742

BIOGRAPHIES

Arata Masuda, a professor of mechanical engineering in Kyoto Institute of Technology, received his Ph.D degree in mechanical engineering from Kyoto Institute of Technology in 1999, BS from Kyoto University in 1990. His research has been in the area of smart structures, structural health monitoring, energy harvesting, vibration control, and system identification.

Konosuke Takashima received the B.Sc. degree in mechanical engineering from the Kyoto Institute of Technology (School of Science and Technology) in 2022. He is currently enrolled in the Division of Mechanophysics, Kyoto Institute of Technology. He is conducting research on the use of physical reservoir computing for new structural health monitoring.